PHYSICAL REVIEW B VOLUME 45, NUMBER 3 15 JANUARY 1992-I

Electronic contributions to scanning-tunneling-microscopy images of an annealed β-SiC(111) surface

M.-H. Tsai, C. S. Chang, John D. Dow, and I. S. T. Tsong
Deparment of Physics, Arizona State University, Tempe, Arizona 85287-1504
(Received 15 July 1991)

The reconstruction of the cubic β-SiC(111) surface was studied after annealing at $\sim 1200\,^{\circ}\mathrm{C}$. The surface consistently showed a $6\sqrt{3}\times 6\sqrt{3}$ geometry when measured by low-energy electron diffraction (LEED) and a 6×6 geometry when imaged by scanning tunneling microscopy (STM). To resolve the discrepancy, we carried out first-principles calculations of the electronic structure of a surface model in which a graphite monolayer was incommensurately grown on top of the Si-terminated β-SiC(111) surface. The calculated energy band and density-of-states diagrams provide an explanation to the observed differences in LEED and STM results. They also explain the voltage-dependent contrast-reversal phenomenon observed in the STM images of the annealed surface.

I. INTRODUCTION

Scanning-tunneling-microscopy (STM) images are known to sample the local density of electronic states near the Fermi level at a surface. In certain cases, these images can be associated with the atomic geometry of the surface, the most well known of which is the Si(111)-7×7,[1] provided that the surface electronic structure is closely tied to individual surface atoms. In other cases, image interpretations are not so straightforward, e.g., in Si(111)-($\sqrt{3}\times\sqrt{3}$)Al,[2] O on GaAs (110),[3] and Si(111)-($\sqrt{3}\times\sqrt{3}$)Ag.[4,5] Nevertheless, in the majority of cases, STM images do reflect the surface geometry and periodicity shown in LEED patterns. In the course of our studies on the reconstructions of the cubic β-SiC(111) surface,[6,7] however, we found a disagreement between the surface geometry determined by STM and that determined by LEED. STM images show a 6×6 geometry while the LEED pattern indicates a $6\sqrt{3}\times 6\sqrt{3}$ geometry. To explain this discrepancy, we have invoked a model originally proposed by van Bommel, Crombeen, and Van Tooren.[8] Three successive carbon layers of β-SiC, after evaporation of silicon by annealing to $1200\,^{\circ}\mathrm{C}$, collapse into one single layer of carbon atoms with a surface density of 3.67×10^{15} atoms cm^{-2}, very close to the density of a graphite monolayer of 3.80×10^{15} atoms cm^{-2}. This layer of carbon atoms then have only to be displaced over small distances to form a graphite layer. The $6\sqrt{3}\times 6\sqrt{3}$ LEED pattern is due to multiple scattering from the graphite monolayer on top of the Si-terminated β-SiC(111) surface.[7,8]

In this paper, we present first-principles calculations of the electronic structure of the annealed β-SiC(111) surface based on the above model in order to explain the 6×6 geometry observed in STM images. Because of the large number of atoms involved in a unit cell, calculations were carried out for the graphite monolayer and the Si-terminated β-SiC(111) surface separately. A comparison of the density of states of these two surfaces is shown to produce the 6×6 geometry.

II. EXPERIMENT

A description of our STM with its associated scanning tunneling spectroscopy (STS) system has been given previously.[6,7] The (111) surfaces of cubic β-SiC monocrystalline films were grown on the Si-terminated (0001) surface of hexagonal α-SiC substrates by the technique of chemical vapor deposition (CVD).[9] Prior to tunneling, the sample surface was annealed to $\sim 1200\,^{\circ}\mathrm{C}$ for 1 min to eliminate the surface oxide layer. After this treatment, the surface consistently showed a $6\sqrt{3}\times 6\sqrt{3}$ LEED pattern, in agreement with the results of van Bommel, Crombeen, and Van Tooren.[8] All STM images of the annealed surface were acquired at a pressure of $\leq 1\times 10^{-10}$ Torr at room temperature.

III. RESULTS

Figure 1 shows voltage-dependent scans of the same region on the annealed β-SiC(111) surface. The surface shows a 6×6 geometry with a unit-cell edge of ~ 19 Å, which is approximately six times the unit-cell edge of 3.1 Å of the β-SiC(111)-(1×1) bulk-terminated surface. The images (a) and (b) of Fig. 1 were taken simultaneously on the same area with the tip biased at $+3.7$ V when scanning from left to right and biased at -3.7 V when scanning from right to left. The hysteresis in the scans was small and had been corrected in the images shown here. The most remarkable feature in these two scans is the occurrence of a contrast reversal. The honeycomb pattern in the filled-state image (a) turns into a centered-hexagon array in the empty-state image (b). The minima of the honeycombs in (a) coincide exactly, as far as the experiment can tell, with the maxima of the centered hexagons in (b). Each honeycomb minimum and each hexagon maximum has a diameter of ~ 12 Å, clearly much larger than the size of a single atom.

Figures 2(a) and 2(b) show filled-state and empty-state images taken with tip biases of $+3$ and -3 V, respectively, on the same area. While the corrugations of filled-

 ©1992 The American Physical Society

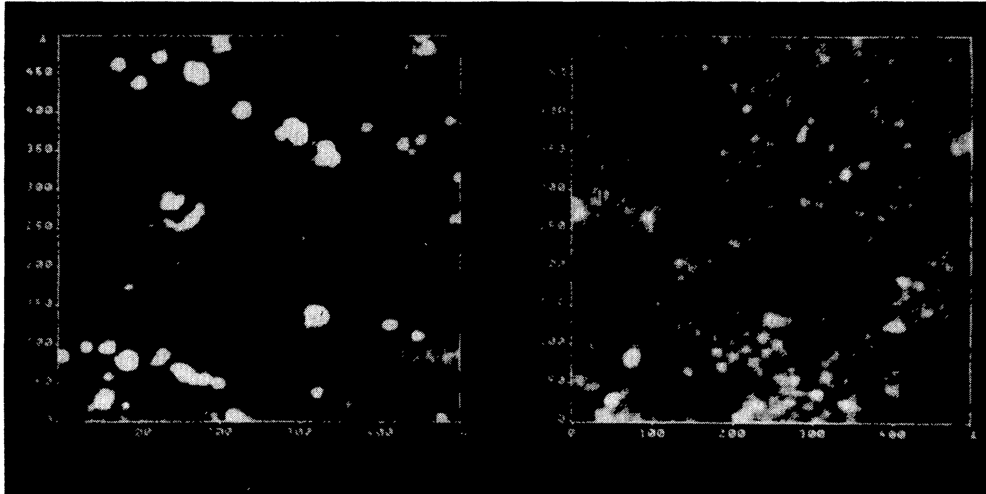

FIG. 1. STM images of the β-SiC(111) surface after annealed at temperature ~1200 °C. Scan area is 500×500 Å^2. (Vertically, 1 div=50 Å; horizontally, 1 div=100 Å.) Tunneling current =1 nA. (a) Filled-state image at tip bias V_t=3.7 V, and (b) empty-state image at tip bias V_t=−3.7 V.

state image (a) appear unchanged compared to the corresponding image in Fig. 1(a), the corrugations in the empty-state image (b) have diminished considerably. In Fig. 3, we plot the corrugation as a function of tip bias for images taken at different biases. It is obvious that the corrugations at positive tip bias, i.e., filled-state images, remain relatively constant, while those at negative bias, i.e., empty-state images, decrease as the tip bias decreases. In fact, at tip bias less than −2.5 V, the corrugations almost completely disappear.

IV. DISCUSSION

We have previously reported[7] the use of STM and STS to show that, upon annealing to 1200 °C, a graphite layer is incommensurately grown on top of the Si-terminated β-SiC(111) surface. Our result agrees with previous results obtained by other workers using LEED, Auger electron spectroscopy, x-ray photoemission spectroscopy, and electron-energy-loss spectroscopy[8,10–12] on hexagonal α-SiC(0001) surfaces which are, of course, equivalent to the cubic β-SiC(111) surface. In Fig. 4, we have drawn a graphite mesh with a periodicity (or unit-cell edge) of 2.46 Å over a Si bulk-terminated (1×1) surface of β-SiC(111) with a periodicity of 3.1 Å. The positions where the top C atoms coincide exactly with the Si atoms underneath are marked with circles and labeled A, B, C, D, E, and F. These positions give rise to the $6\sqrt{3}\times6\sqrt{3}$ geometry observed by LEED since the unit-cell edges, AE and CE, each have a length of 13 graphite hexagons, i.e., 13×2.46 Å, which is virtually identical to $6\sqrt{3}\times3.1$ Å. Around each of the positions A–F, there are three pairs of C and Si atoms at apexes of the dotted triangle lying very close to each other, i.e. within 0.3 Å laterally. The position G, given by the dotted circle in Fig. 4, does not have any C atoms directly above a Si atom. Six C atoms on the dotted circle, however, are lying very close to six Si atoms. We speculated[7] that

FIG. 2. STM images of the β-SiC(111) surface after annealed at temperature ~1200 °C. Scan area is 500×500 Å^2. Tunneling current is 1 nA. (a) Filled-state image at tip bias V_t=3 V, and (b) empty-state image at tip bias V_t=−3 V.

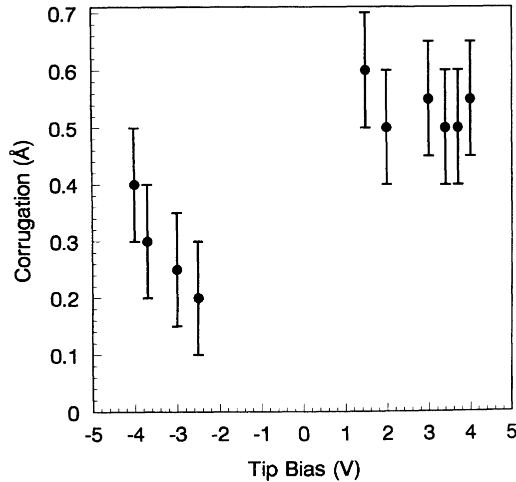

FIG. 3. Z corrugation plotted as a function of tip bias taken from STM images of the β-SiC(111) surface.

ABGF forms the 6×6 geometry observed by STM. To explain the contrast reversal phenomenon as the tip bias is reversed, we need detailed knowledge of the electronic structure of the surface.

To calculate the 6×6 surface directly is beyond the capability of a first-principles method because each unit cell contains hundreds of atoms. Thus, our approach to solve the problem is to model the system separately by a graphite monolayer and a Si-terminated β-SiC(111) surface.

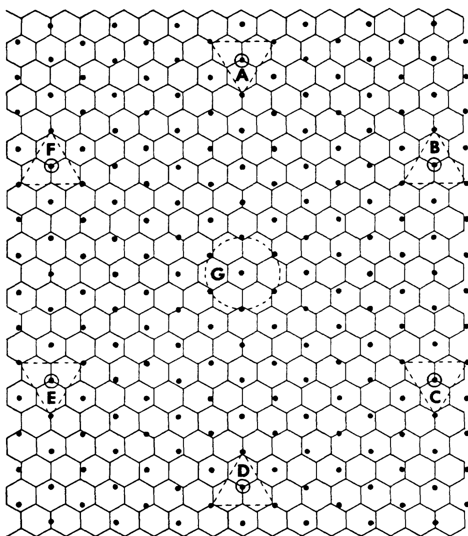

FIG. 4. A model of a graphite monolayer (represented by honeycombs) incommensurately grown on the (1×1) Si-terminated β-SiC(111) surface (represented by dots). The dashed triangles, denoted A, B, C, D, E, and F, indicate positions where the graphite atoms at the centers of triangles coincide exactly with the Si atoms in the second layer, and those graphite atoms at the apexes almost coincide with the Si atoms underneath. The dashed circle, G, outlines positions where the graphite and Si atoms nearly coincide. The unit-cell spacing is 2.46 Å for graphite and 3.1 Å for the (1×1) Si-terminated surface.

We use the first-principles pseudofunction (PSF) method[13] in a local-density approximation (LDA) (Ref. 14) to calculate the electronic structures of the graphite monolayer and the β-SiC(111) surface.

For the β-SiC(111) surface, an isolated eight atomic-layer (or four double-layer) slab model is used. Because of the double-layer nature of β-SiC(111), one surface of the crystal is terminated in Si and the opposite surface is terminated in C. Each C atom on the opposite surface of the slab is attached with a hydrogen atom to saturate the dangling bond in order to prevent charges from transferring back and forth between the two surfaces of the slab, thus making convergence possible. We use the experimental lattice parameter of 4.3596 Å,[15] and the bulklike crystal structure for the β-SiC. For the graphite monolayer, we also use an isolated slab model. The lattice parameter is 2.456 Å as given in the literature.[16,17] The special k-point scheme of Cunningham[18] for a two-dimensional hexagonal lattice is used to approximate the integration over the first Brillouin zone in calculating the self-consistent charge densities and potential for both cases. We use one special k point for β-SiC and six special k points for graphite.

Calculated energy bands for the β-SiC(111) and the graphite monolayer are shown in Figs. 5 and 6, respectively. In both figures, energies are given relative to the vacuum level. In Fig. 5, there is a very flat half-filled Si dangling-bond energy band around -5 eV inside the fundamental energy gap, giving rise to a very strong peak in the partial density of states of the Si surface atoms as shown in Fig. 7. The calculated energy gap is 1.45 eV, which is about half of the experimental value 2.3 eV.[15] This discrepancy is well known to be the result of a deficiency of the LDA.[19] The Fermi level lies within the dangling-bond state band and is 4.8 eV below the vacuum level, i.e., the work function is 4.8 eV.

For the graphite monolayer, the energy bands shown in Fig. 6 are similar to those of Tatar and Rabii[16] using a modified Korringa-Kohn-Rostoker approach for three-dimensional graphite and also to those of Posternak

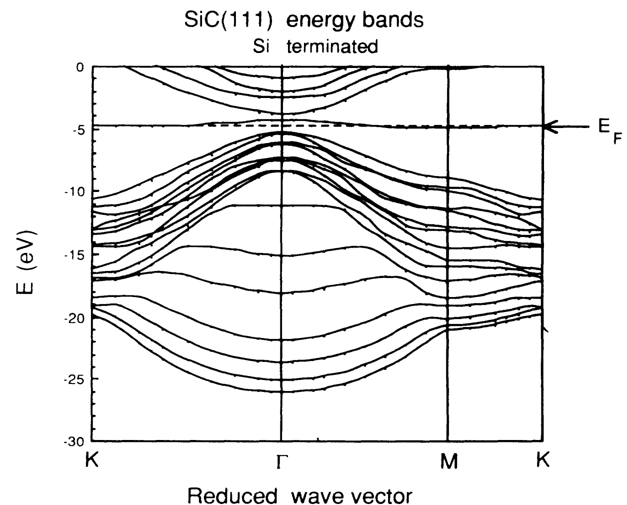

FIG. 5. Calculated energy-band diagram of the Si-terminated surface of β-SiC(111). Dashed line indicates the Fermi level.

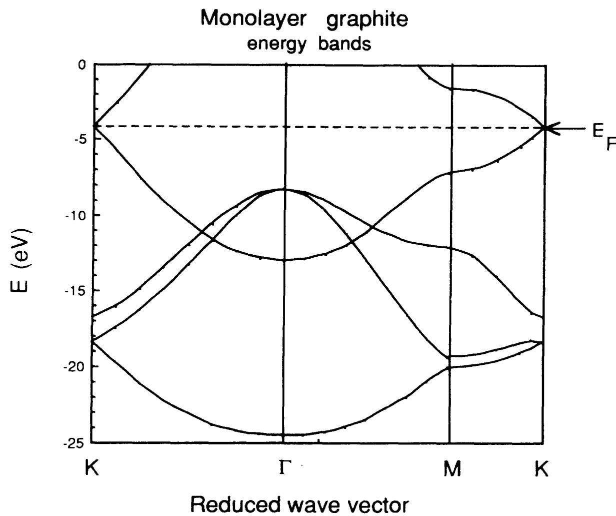

FIG. 6. Calculated energy-band diagram of the graphite monolayer.

et al.[20] using the full-potential linearized augmented-plane-wave (FLAPW) method for a graphite monolayer. We obtain a work function of 4.2 eV for the graphite monolayer compared to 5.02 eV obtained by Posternak *et al.*[20] Previous calculated work functions scatter over a range between 5.0 and 8.0 eV.[20,21] The experimental work function for bulk graphite is 5.0 eV.[15] The work function for the bulk material is expected to be higher than that for the monolayer because the escaping electron experiences an extra attractive potential from the inner layers despite the fact that the couplings between graphite layers are weak. Thus our calculated work function for the graphite monolayer appears reasonable.

The contributions to the STM images can be approximately divided into two parts, one from the Si dangling-bond states and the other from the graphite electronic states. The Si dangling-bond band is half filled. However, the band and the corresponding density of states are not symmetrical with respect to the Fermi level as indicated in Fig. 5. Referring to Fig. 5, the filled-state part, i.e., the part below the Fermi level (dashed line), is extremely flat and is in the large wave-vector region. In contrast, the empty-state part surrounding the Γ point has a more pronounced curvature, i.e., larger energy spread, and has smaller wave vectors. Thus the empty states are more delocalized and the corresponding density of states is much smaller than that for the filled states. Because of this, one expects the contribution of the Si dangling-bond states to be larger for filled-state images (i.e., positive tip bias) than for empty-state images (negative tip bias).

Since the work function for the graphite monolayer is smaller than that for the Si-terminated β-SiC(111), there is a net charge transfer from the graphite to the β-SiC. The graphite Fermi level is located at the π band, which is composed solely of p_z orbitals; here, z is the coordinate normal to the surface. When there is a Si atom directly beneath or close to a C atom in the graphite layer, the charge transfer from the C atom to underneath the Si atom will be maximum. Otherwise, the charge transfer will be small due to the highly directional p_z orbital. We write $\rho_1(E)$ for the density of states of those C atoms which have a Si atom directly underneath or close to them, i.e., C atoms in regions $A-G$ in Fig. 4, and $\rho_2(E)$ for the density of all other C atoms. The density of states for bulk graphite has been given by Tatar and Rabi.[16] Since the energy bands of the graphite monolayer are similar to those of bulk graphite, the density of states for them will be similar. Within about 2.5 eV of the Fermi level, the density of states is approximately parabolic,[16] which is shown in Fig. 8. Thus

$$\rho_2(E) \approx K(E-E_F)^2 , \quad (1)$$

where K is a proportionality constant.

For those C atoms with a Si atom underneath or in close proximity, charge transfer from C to Si atoms will shift the density-of-states curve downwards by an amount δ as shown in Fig. 8, resulting in an attractive electrostat-

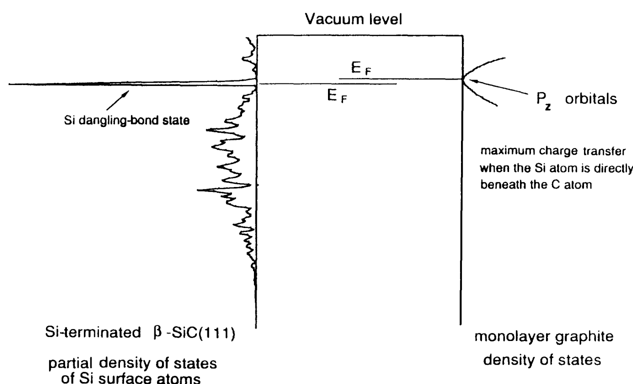

FIG. 7. Calculated partial density of states for the Si-terminated surface of β-SiC(111) and for the graphite monolayer from Ref. 16. The Fermi levels with respect to each other are shown below the vacuum level.

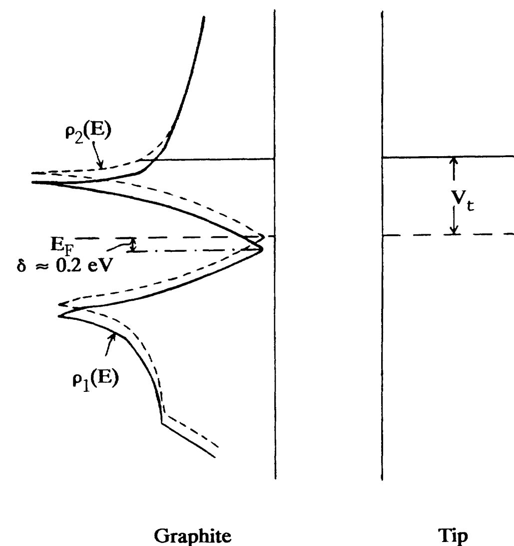

FIG. 8. Shift in the density of states of the graphite monolayer (Ref. 16) as a result of charge transfer. The number of states samples by different tip biases is also shown.

ic potential. δ has a positive value in energy units. Then

$$\rho_1(E) \approx K(E-E_F+\delta)^2 \ . \tag{2}$$

For tip bias V_t, let $N_1(E_F,V_t)$ and $N_2(E_F,V_t)$ be the numbers of states between E_F and E_F-eV_t for the kinds of C atoms mentioned earlier. Let ΔN be the difference in the number of states sampled by STM from the two kinds of C atoms on the surface, which in turn gives rise to the contrast observed in Figs. 1 and 2. Hence

$$\Delta N = N_1(E_F,V_t) - N_2(E_F,V_t) \ . \tag{3}$$

We write ΔN^+ for $V_t > 0$ or positive tip bias (sampling filled states), and ΔN^- for $V_t < 0$ or negative tip bias (sampling empty states). From Eqs. (1)–(3), we now have

$$\Delta N^+ = \int_{E_F-eV_t}^{E_F} K\rho_1(E)dE - \int_{E_F-eV_t}^{E_F} K\rho_2(E)dE \tag{4}$$

giving

$$\Delta N^+ \approx -K[(eV_t)^2\delta - (eV_t)\delta^2] \tag{5}$$

or

$$\Delta N^+ \approx -Ke^2V_t^2\delta \ .$$

Similarly,

$$\Delta N^- = \int_{E_F}^{E_F+e|V_t|} K\rho_1(E)dE - \int_{E_F}^{E_F+e|V_t|} K\rho_2(E)dE \ , \tag{6}$$

$$\Delta N^- \approx Ke^2V_t^2\delta \ . \tag{7}$$

The opposite signs in Eqs. (5) and (7) explain the contrast reversal observed in the (a) and (b) images in Figs. 1 and 2.

In Eq. (7) for empty-state images, the contrast has a V_t^2 dependence, which means the contrast is large for large negative tip bias, but decreases rapidly as the bias decreases. This may explain the corrugation dependence shown in Fig. 3, i.e., the empty-state images show little corrugation for small negative tip bias, and the corrugation only becomes pronounced at large biases. Such a dependence is not observed for filled-state images because of the influence of the Si dangling-bond states.

As we have discussed earlier, the empty Si dangling-bond states are more delocalized or diffused. Their contribution relative to that of graphite states includes a geometric factor of roughly $e^{-2d\sqrt{\phi}}$, where ϕ is the work function in Ry and d is the distance between the graphite layer and the Si surface layer in Bohr radius. This factor has an order of 10^{-2}, which implies a negligible contribution to the empty-state images. On the other hand, for positive tip biases measuring the filled states, the very strong localized Si dangling-bond states should be able to compensate for the deficiency caused by the geometric factor and contribute significantly to the filled-state images. This may be the reason why the corrugations in the filled-state images in Figs. 1 and 2 are insensitive to changes in tip bias.

V. CONCLUSIONS

The discrepancy between the 6×6 STM geometry and the $6\sqrt{3}\times6\sqrt{3}$ LEED pattern for the β-SiC(111) surface can be explained by an incommensurate graphite monolayer grown on the Si-terminated β-SiC(111) surface during the annealing process. The contrast reversal phenomenon observed in the STM images at opposite tip biases can be explained by the different electronic contributions from graphite states of those C atoms with Si atoms directly (or almost directly) underneath and those without. The Si dangling-bond states contribute significantly to the corrugations observed in the filled-state images.

ACKNOWLEDGMENTS

We thank Y. C. Wang and R. F. Davis of North Carolina State University for providing the β-SiC(111) single crystals. We also thank U. Knipping for improvements in the STM imaging and spectroscopy software. This work was supported by the U.S. Army Research Office under Contracts DAAL 03-88-K-0098 and DAAL 03-91-G-0054.

[1] G. Binnig, H. Rohrer, Ch. Gerber, and E. Weibel, Phys. Rev. Lett. **50**, 120 (1982).
[2] R. J. Hamers and J. E. Demuth, Phys. Rev. Lett **60**, 2527 (1988).
[3] J. A. Stroscio, R. M. Feenstra, D. M. Newns, and A. P. Fein, J. Vac. Sci. Technol. A **6**, 499 (1988).
[4] R. J. Wilson and S. Chiang, Phys. Rev. Lett. **58**, 369 (1987).
[5] E. J. van Loenen, J. E. Demuth, R. P. Tromp, and R. J. Hamers, Phys. Rev. Lett. **58**, 373 (1987).
[6] C. S. Chang, N. J. Zheng, I. S. T. Tsong, Y. C. Wang, and R. F. Davis, J. Vac. Sci. Technol. B **9**, 681 (1991).
[7] C. S. Chang, I. S. T. Tsong, Y. C. Wang, and R. F. Davis, Surf. Sci. **256**, 354 (1991).
[8] A. J. van Bommel, J. E. Crombeen, and A. van Tooren, Surf. Sci. **48**, 463 (1975).
[9] H. S. Kong, J. T. Glass, and R. F. Davis, J. Mater. Res. **4**, 204 (1989).
[10] R. Kaplan, Surf. Sci. **215**, 111 (1989).
[11] L. Muehlhoff, W. J. Choyke, M. J. Bozack, and J. T. Yates, Jr., J. Appl. Phys. **60**, 2842 (1986).
[12] K. Miyosi and D. H. Buckley, Appl. Surf. Sci. **10**, 357 (1982).
[13] R. V. Kasowski, M.-H. Tsai, T. N. Rhodin, and D. D. Chambliss, Phys. Rev. B **34**, 2656 (1986).
[14] L. Hedin and B. I. Lundqvist, J. Phys. C **4**, 2064 (1971).
[15] Handbook of Chemistry and Physics, 71st ed., edited by D. R. Lide (CRC, Boca Raton, FL, 1990–1991); B. Robrieux, R. Faure, and J. P. Dussauley, C. R. Acad. Sci. Ser. B **278**(14), 659 (1974).
[16] R. C. Tatar and S. Rabii, Phys. Rev. B **25**, 4126 (1982).
[17] D. Sands, *Introduction to Crystallography* (Benjamin-

Cummings, Reading, MA, 1969).
[18]S. L. Cunningham, Phys. Rev. B **10**, 4988 (1974).
[19]M. S. Hybertsen and S. G. Louie, Phys. Rev. B **34**, 5390 (1986).
[20]M. Posternak, A. Baldereschi, A. J. Freeman, E. Wimmer, and M. Weinert, Phys. Rev. Lett. **50**, 761 (1983).
[21]A. Zunger, Phys. Rev. B **17**, 626 (1978), and references therein.

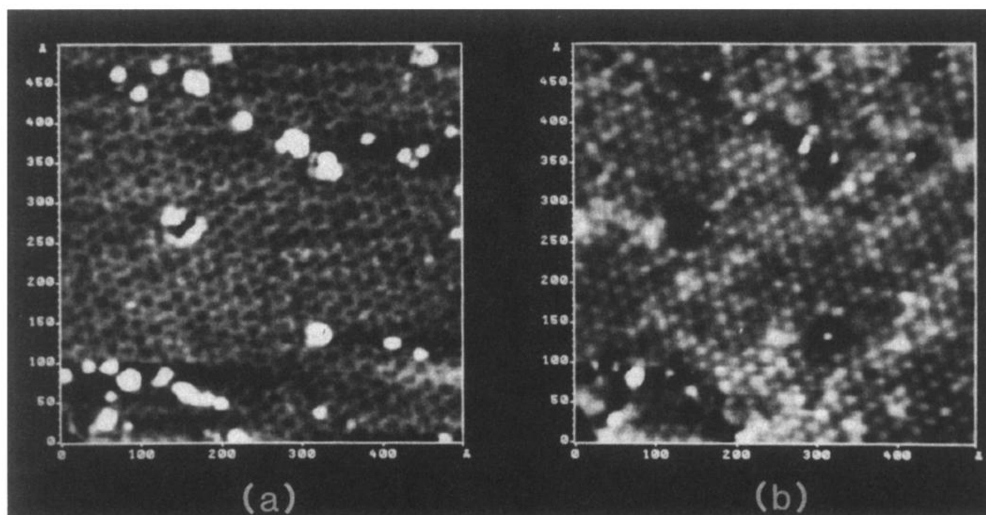

FIG. 1. STM images of the β-SiC(111) surface after annealed at temperature $\sim 1200\,^{\circ}\mathrm{C}$. Scan area is 500×500 Å^2. (Vertically, 1 div$=50$ Å; horizontally, 1 div$=100$ Å.) Tunneling current $=1$ nA. (a) Filled-state image at tip bias $V_t = 3.7$ V, and (b) empty-state image at tip bias $V_t = -3.7$ V.

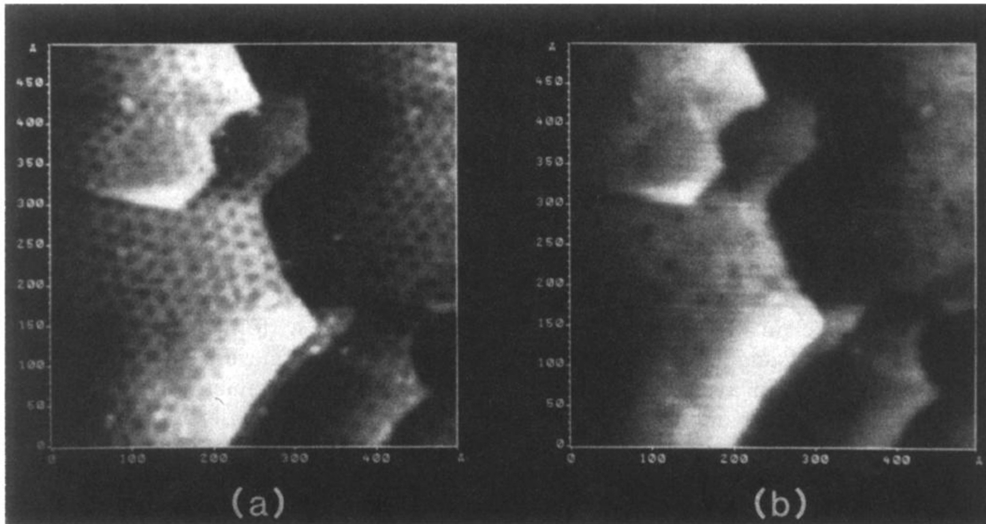

FIG. 2. STM images of the β-SiC(111) surface after annealed at temperature $\sim 1200\,^{\circ}\mathrm{C}$. Scan area is 500×500 Å^2. Tunneling current is 1 nA. (a) Filled-state image at tip bias $V_t = 3$ V, and (b) empty-state image at tip bias $V_t = -3$ V.